Sciencexpress Reports

Ice Shelf Melting Around Antarctica

E. Rignot,[1,2]* S. Jacobs,[3] J. Mouginot,[1] B. Scheuchl[1]

[1]Department of Earth System Science, University of California, Irvine, CA 92697, USA. [2]Jet Propulsion Laboratory, Pasadena, CA 91109, USA. [3]Lamont-Doherty Earth Observatory, Columbia University, Palisades, NY 10964, USA.

*Corresponding author. E-mail: erignot@uci.edu

We compare the volume flux divergence of Antarctic ice shelves in 2007–2008 with 1979–2010 surface accumulation and 2003–2008 thinning to determine their rates of melting and mass balance. Basal melt of 1325 ± 235 gigatons per year (Gt/year) exceeds a calving flux of 1089 ± 139 Gt/year, making ice shelf melting the largest ablation process in Antarctica. The giant cold-cavity Ross, Filchner, and Ronne ice shelves covering two-thirds of the total ice shelf area account for only 15% of net melting. Half of the meltwater comes from 10 small, warm-cavity southeast Pacific ice shelves occupying 8% of the area. A similar high melt/area ratio is found for six East Antarctic ice shelves, implying undocumented strong ocean thermal forcing on their deep grounding lines.

The Antarctic Ice Sheet and its 58-m sea level equivalent (*1*) is buttressed along most of its periphery by floating extensions of land ice called ice shelves and floating ice tongues (Fig. 1). Ice shelves cover an area >1.561 million km^2, comparable in size to the Greenland Ice Sheet, and fringe 75% of Antarctica's coastline while collecting 20% of its snowfall over 11% of its area (*2*, *3*). These features are nourished by the inflow of continental ice from grounded glaciers, surface accumulation and freezing of marine ice on their undersides. They lose mass to iceberg calving and basal melting along with topside sublimation and wind drift. Ice shelves exert considerable control on glacier stability and Antarctic Ice Sheet mass balance (*4*–*6*) and play significant roles in ocean stratification and bottom water formation (*7*).

The traditional view of ablation from Antarctic ice shelves has been that it occurs mostly by iceberg calving, with basal melting only contributing 10 to 28% of the total mass loss (*3*–*6*). Estimates of ice shelf meltwater production derived from oceanographic data (*8*–*10*, e.g.) are impractical for synoptic circumpolar coverage. Numerical simulations of ice-ocean interactions extend from individual ice shelves to circumpolar models at various resolutions, but comparisons with observations are limited, and estimates of total ice shelf meltwater production have varied from 357 to 1,600 gigatons per year (1 Gt = 10^{12} kg) (*3*, *7*, *11*). Glaciological estimates have focused on few ice shelves (*6*, *12*, *13*) or near a fraction of glacier grounding lines (*14*) due to incomplete velocity and thickness mapping.

Here we present more accurate, higher-resolution glaciological estimates of ice shelf melting around the entire continent. At any point on an ice shelf of thickness H and velocity vector $\mathbf{v}$, the rate of ice shelf thickening $\partial H/\partial t$ equals the sum of net surface mass balance *SMB* minus net basal melting B minus the lateral divergence in volume flux $H\mathbf{v}$ (*15*). A negative value of B indicates the freeze-on of marine ice. The calculation of volume flux divergence on a point per point basis yields the distribution of freeze/melt (Fig. 1). The integration of the total inflow and outflow within the ice shelf perimeters yields the area-average melt rate and total melt water production (Table 1).

For *SMB*, we use output products from the Regional Atmospheric and Climate Model RACMO2 (*16*), which is forced at the lateral boundary and sea surface by global reanalyses of the European Centre for Medium-Range Weather Forecasts. RACMO2 includes surface melt water retention due to refreezing, evaporation, wind drift and sublimation. The products have been validated with field data and an error propagation analysis (*17*) to a precision of 7 to 25%, average 10%, depending on location. We use the average *SMB* for the years 1979–2010 to represent a longer-term state.

Ice shelf thickness is from Operation IceBridge (OIB) (*18*, *19*) and BEDMAP-2 (*1*) (fig. S1, supplementary materials). It combines direct measurements from radio echo sounding, with indirect estimates from altimetry-derived ice shelf surface elevation assuming hydrostatic equilibrium with a nominal precision of 15 to 50 m (*20*). Flux gates are selected at the location of Interferometric Synthetic Aperture Radar (InSAR)–derived grounding lines, which are more precise than derived from photogrammetric techniques or visible imagery (*21*), with accompanying impacts on estimates of volume fluxes. Ice-front flux gates are at the seaward limit of the volume flux data, within 1 to 3 km of ice-front positions digitized from a 150-m spacing mosaic of Advanced Land Observing System (ALOS) Polarimetric SAR (PALSAR) data for the years 2007-2008.

Ice shelf flow vector velocities are from InSAR data collected in 2007–2008 and processed at 450 m spacing (*22*). The average precision in speed is 4 m/year and 1.7° in direction (fig. S2). In the absence of vertical shear on floating ice, the surface-derived velocity is equivalent to a depth-averaged velocity. We survey 99.5% of Antarctic ice shelf area in 2007–2008 (Table 1), or 1.554 million km^2, excluding a few smaller ice shelves where ice thickness is not well known (table S1). Drainage boundaries between ice shelves, including the eastern and western Ross, are defined by flow vector direction. Ice rises and islands are excluded from the ice shelf area estimates but included in the *SMB* calculation.

Ice-shelf thickening $\partial H/\partial t$ for the period 2003–2008 is calculated using the procedure in (*23*), with an error dependent on firn depth corrections (fig. S3). The results are combined with *SMB* and the flux divergence to calculate B, with a precision dominated by uncertainties in ice-front thickness and firn depth corrections (table S1). We also calculate the results for $\partial H/\partial t = 0$, i.e., no ice shelf thickness change, to obtain a reference rate B_{ss} corresponding to the amount of freezing or melting that would be required to maintain an ice shelf in "steady state" for 2007–2008 (fig. S4).

The freeze/melt distribution confirms that basal melting is strongest near the grounding zones of major glaciers and along the ice fronts of some of the largest ice shelves, especially Ronne (Fig. 1). Ice shelf melting decreases away from grounding lines and becomes negative (accretion of marine ice) on all large ice shelves and some smaller ice shelves. This general pattern of melting and freezing beneath ice shelves is well understood (*4*–*6*, *15*) and is governed by the Coriolis-influenced transport and vertical mixing of ocean heat, the pressure-dependence of the freezing point of seawater, and the sea floor and cavity morphology. On some large ice shelves, freezing is concentrated on the western sides, consistent with an oceanic circulation during which seawater is first cooled, freshened and made more buoyant by melting.

The highest melt rates are detected in the southeast Pacific sector of the Antarctic Peninsula and West Antarctica, from the northern end of George VI to the western end of Getz Ice Shelf. On slow-moving to nearly-stationary ice shelves like the Wilkins, George VI, Abbot and Sulzberger, basal melting entirely consumes the inflow of individual glaciers within a few km of their grounding zones. High melt rates are also revealed in the grounding zones of the Amery, Moscow University, Shackleton, and Totten in East Antarctica.

In contrast, low melt rates are found under the largest ice shelves, e.g., the Ross West, except near deep grounding lines. Maximum grounding line depth is only 0.9 km under the Ross West but 2.1 km under the Filchner and Ronne, 1.8 km under Ross East, and 2.4 km under the Amery (*1*). Each additional 100 m adds 0.076°C to the thermal driving of seawater that may have started out near the sea surface freezing point. Differences in observed melt rate may also be accentuated by variations in flushing time and tidal activity (*24*).

Total ice inflow and outflow for each ice shelf is summarized in Fig. 1 and Table 1. Ice-front flux is a proxy for, but not identical to, iceberg calving, which occurs at irregular time intervals ranging from years to decades. The higher basal melting near some ice-shelf fronts (*12*, *25*) results from stronger tidal currents and mixing, especially in combination with a shallow water column (*24*), as along the eastern front of Ronne [150 ± 50 m in (*1*) versus 350 ± 100 m for Ross or 500 ± 250 m for Filchner]. Ice-front fluxes may overestimate iceberg calving where near ice front melting is significant and calving is infrequent; conversely, large icebergs may on average be thicker than the ice front, in which case ice front fluxes underestimate calving.

The total ice shelf grounding line inflow of 1,696 ± 146 Gt/year combined with an *SMB* input of 430 ± 81 Gt/year is partitioned into an ice-front flux of 1,089 ± 139 Gt/year and a basal meltwater production of 1,325 ± 235 Gt/year. Basal melting thus accounts for 55 ± 10% of ice shelf mass ablation. The corresponding area-average melt rate of 85 ± 15 cm/year is three times as large as the average *SMB* on ice shelves (28 ± 5 cm) and five times the average *SMB* on grounded ice sheet (16 ± 1 cm) (*16*), illustrating the considerable importance of ocean interactions in freshwater transfers between the ice and ocean.

The grounding line flux of all surveyed ice shelves accounts for 83 ± 7% of the total ice discharge into the Southern Ocean (Table 1). Total Antarctic grounded ice discharge (*26*) is 352 ± 30 Gt/year higher than our grounding line flux because of additional discharge from smaller ice shelves and ice walls that terminate in the ocean (*27*). An equal partitioning of these missing areas between calving and basal melting (see supplementary materials) would increase in-situ meltwater production to 1,500 ± 237 Gt/year and ice-front flux to 1,265 ± 139 Gt/year.

The comparison of basal melting, B (Fig. 1) with steady state melting, B_{ss} (fig. S4, Table 1, and table S1) shows that many ice shelves are near equilibrium ($B \sim B_{ss}$), while some are thickening ($B < B_{ss}$) and others are thinning ($B > B_{ss}$). High basal melting is therefore not synonymous with thinning. Ice shelves with high melt rates can be in a state of mass balance, but meltwater production is 28 ± 9% higher than required to maintain the ice shelves in overall steady state (1037 ± 218). Ice shelves in the Amundsen Sea sector (Pine Island to Getz) contribute 59% of the 287 ± 89 Gt/year imbalance, an attrition rate twice that of their glacier source regions over the same time period (*26*). Similarly, the total imbalance of all Antarctic ice shelves combined is more than twice that of the grounded ice (*26*).

The ratio of calving to melting averages 0.45 ± 0.3, but exhibits significant regional variability (Table 1), with area-average melt rates varying from negative to > 40 m/year. This wide range reflects diverse ocean environments, which include seawater temperature, the depths of troughs and sills that influence the access of oceanic heat to ice shelf cavities, and the sea ice formation and drifts resulting from atmospheric forcing.

Large ice shelves generate a disproportionally small portion of the total ice shelf meltwater despite high production rates in their deep grounding zones and along lengthy ice fronts. The four giants with areas > 100,000 km^2 (Ross East, Ross West, Filchner and Ronne) cover 61% of the total ice shelf area but contribute only 15% of the meltwater at an average rate of 13 cm/year. The low melt rates result from the relatively weak ocean heat source provided by cold shelf waters, in turn leading to substantial marine ice accretion (*28*). Despite areas 3-10 times larger than the Getz, none of the big four ice shelves produce as much meltwater, with the Ross West contributing no net melt. Meltwater from the southeast Pacific-Antarctic sector (George VI through Getz) accounts for 48% of the total meltwater over only 8% of the area, with the Getz being the largest meltwater source in Antarctica during the study period. B averages 5.1 m/year in this region, from a maximum of 43 m/year under the short Ferrigno Glacier tongue, to a minimum of 1.8 m/year beneath the Abbot. That area-average rate may seem low for a warm-cavity Southeast Pacific ice shelf, but the moderate-sized, shallow-draft Abbot (*29*) ranks 8th overall in meltwater production, while maintaining a positive mass balance ($B < B_{ss}$).

Meltwater production from several small East Antarctic ice shelves in the Wilkes Land sector is larger than expected. Area-average melt rates from Dibble through Vincennes (4-11 m/year) are comparable to Amundsen Sea ice shelf rates from Crosson through Land (4-11 m/year), while meltwater produced by Shackleton and West (73 and 27 Gt/year) rivals that from Thwaites and Sulzberger (98 and 18 Gt/year). Except for the region from 140-150°W where the Mertz and Ninnis float in cold shelf waters, oceanographic data are sparse along the Wilkes Land coastline. "Modified" warm deep water at a temperature near 0°C has been reported 40 km south of the continental shelf break northeast of Totten (*30*). By analogy with observations in the Amundsen Sea, our results suggest the presence of seawater at similar temperatures under several East Antarctic ice shelves. Even zero-degree seawater at outer continental shelf depths could expose ice shelves with deep grounding lines like the Totten (2.2 km), Moscow (2.0 km) and Shackleton (1.8 km) to temperatures more than 3°C above their melting points. To evaluate the impact of these warm deep waters on ice shelf melting, more information is needed about their spatial and temporal variability on the outer shelf, and links via glacially scoured troughs to the vulnerable glacier grounding lines.

Our glaciological estimates are generally consistent with recent results from high-resolution ocean models in the Amundsen, Bellingshausen, and Weddell Seas (*29*, *31–33*) (see supplementary materials), but melting of the largest ice shelves is notably less here than in circumpolar models (*7*, *11*). Discrepancies between model results and observations have been attributed to deficiencies in atmospheric forcing, the representation of sea ice cover, the smoothing of bottom topography and assumptions regarding cavity shape. Some models yield annual cycles and decadal variability (*29*) that can now be compared for specific periods with glaciological measurements, which need to be extended in time.

Our results indicate that basal melting accounts for a larger fraction of Antarctic ice shelf attrition than previously estimated. These improved glaciological estimates not only provide more accurate and detailed reference values for modeling, but a baseline for similar future studies. Ice shelf melt water production exhibits a complex spatial pattern around the continent, with an outsized contribution of smaller, fast-melting ice shelves in both West and East Antarctica. Warm-cavity ice shelves along the southeast Pacific coastline, predicted and observed to be sensitive to ocean warming and circulation strength (*9*, *34*), are thinning and losing mass rapidly. Nearly half of the East Antarctic ice shelves are also thinning, some due to probable exposure to "warm" seawater, with connections to ice drainage basins grounded below sea level.

Continued observations of ice shelf velocity and thickness change, along with more detailed information on cavity shape, seafloor topography and atmospheric and oceanic forcing variability are critical to understand the temporal variability and evolution of Antarctic ice shelves. Continued warming of the ocean will slowly increase ice shelf thinning, but if major shifts in sea ice cover and ocean circulation tip even large ice shelf cavities from cold to warm (*35*), there could be major changes in ice shelf and thus ice sheet mass balance.

References and Notes

1. P. Fretwell *et al*., Bedmap2: Improved ice bed, surface and thickness datasets for Antarctica. *The Cryosphere* **7**, 375 (2013). doi:10.5194/tc-7-375-2013
2. C. W. Swithinbank, *Satellite Image Atlas of Glaciers of the World: Antarctica*, R. S. Williams, J. G. Ferrigno, Eds. (USGS Prof. Paper 1386-B, 1988).
3. N. I. Barkov, *Ice Shelves of Antarctica* (New Delhi, NY, Amerind Pub. Co., 1985).
4. R. LeB. Hooke, *Principles of Glacier Mechanics* (Cambridge University Press, Cambridge, 2005).
5. K. M. Cuffey, W. S. B. Paterson, *The Physics of Glaciers* (Elsevier, Burlington, MA, ed. 4, 2010).
6. S. S. Jacobs, H. H. Hellmer, C. S. M. Doake, A. Jenkins, R. M. Frolich, Melting of ice shelves and the mass balance of Antarctica. *J. Glaciol.* **38**, 375 (1992).
7. H. H. Hellmer, Impact of Antarctic ice shelf basal melting on sea ice and deep ocean properties. *Geophys. Res. Lett.* **31**, L10307 (2004). doi:10.1029/2004GL019506
8. A. Jenkins, S. S. Jacobs, Circulation and melting beneath George VI Ice Shelf, Antarctica. *Geophys. Res. Lett.* **113**, (C4), C04013 (2008). doi:10.1029/2007JC004449
9. S. S. Jacobs, A. Jenkins, C. F. Giulivi, P. Dutrieux, Stronger ocean circulation and increased melting under Pine Island Glacier ice shelf. *Nature Geosc.* **4**, 519 (2011). doi:10.1038/ngeo1188
10. A. Foldvik, T. Gammelsrod, E. Nygaard, S. Osterhus, Current measurements near Ronne Ice Shelf: Implications for circulation and melting. *J. Geophys. Res. Oceans* **106**, (C3), 4463 (2001). doi:10.1029/2000JC000217
11. R. Timmermann, Q. Wang, H. H. Hellmer, Ice-shelf basal melting in a global finite-element sea-ice/ice-shelf/ocean model. *Ann. Glaciol.* **53**, 303 (2012). doi:10.3189/2012AoG60A156
12. I. Joughin, L. Padman, Melting and freezing beneath Filchner-Ronne Ice Shelf, Antarctica. *Geophys. Res. Lett.* **30**, 1477 (2003). doi:10.1029/2003GL016941
13. J. Wen *et al*., Basal melting and freezing under the Amery Ice Shelf, East Antarctica. *J. Glaciol.* **56**, 81 (2010). doi:10.3189/002214310791190820
14. E. Rignot, S. S. Jacobs, Rapid bottom melting widespread near Antarctic Ice Sheet grounding lines. *Science* **296**, 2020 (2002). doi:10.1126/science.1070942 Medline
15. A. Jenkins, C. S. M. Doake, Ice ocean interaction on Ronne Ice Shelf, Antarctica. *J. Geophys. Res.* **96**, (C1), 791 (1991). doi:10.1029/90JC01952
16. J. T. M. Lenaerts *et al*., Modeling drifting snow in Antarctica with a regional climate model: 1. Methods and model evaluation. *J. Geophys. Res.* **117**, (D5), D05108 (2012). doi:10.1029/2011JD016145
17. E. Rignot *et al*., Recent mass loss of the Antarctic Ice Sheet from dynamic thinning. *Nat. Geosci.* **1**, 106 (2008). doi:10.1038/ngeo102
18. C. Allen, IceBridge MCoRDS L2 Ice Thickness. Boulder, Colorado USA: NASA DAAC at the National Snow and Ice Data Center (2010).
19. D. D. Blankenship, S. Kempf, D. Young, IceBridge HiCARS 2 L2 Geolocated Ice Thickness. Boulder, Colorado USA: NASA DAAC at the National Snow and Ice Data Center (2012).
20. J. A. Griggs, J. L. Bamber, Antarctic ice-shelf thickness from satellite radar altimetry. *J. Glaciol.* **57**, 485 (2011). doi:10.3189/002214311796905659
21. E. Rignot, J. Mouginot, B. Scheuchl, Antarctic grounding line mapping from differential satellite radar interferometry. *Geophys. Res. Lett.* **38**, L10504 (2011). doi:10.1029/2011GL047109
22. E. Rignot, J. Mouginot, B. Scheuchl, Ice flow of the Antarctic ice sheet. *Science* **333**, 1427 (2011). doi:10.1126/science.1208336 Medline
23. H. D. Pritchard *et al*., Antarctic ice-sheet loss driven by basal melting of ice shelves. *Nature* **484**, 502 (2012). doi:10.1038/nature10968 Medline
24. K. Makinson, P. R. Holland, A. Jenkins, K. Nicholls, D. M. Holland, Influence of tides on melting and freezing beneath Filchner Ronne Ice Shelf, Antarctica. *Geophys. Res. Lett.* **38**, L06601 (2011). doi:10.1029/2010GL046462
25. H. J. Horgan, R. T. Walker, S. Anandakrishnan, R. B. Alley, Surface elevation changes at the front of the Ross Ice Shelf: Implications for basal melting. *J. Geophys. Res.* **116**, (C2), C02005 (2011). doi:10.1029/2010JC006192
26. A. Shepherd *et al*., A reconciled estimate of ice-sheet mass balance. *Science* **338**, 1183 (2012). doi:10.1126/science.1228102 Medline
27. S. Neshyba, E. G. Josberger, On the estimation of Antarctic iceberg melt rate. *J. Phys. Oceanogr.* **10**, 1681 (1980). doi:10.1175/1520-0485(1980)010<1681:OTEOAI>2.0.CO;2
28. K. Grosfeld *et al*., Marine ice beneath Filchner Ice Shelf: Evidence from a multi-disciplinary approach. *Antarct. Res. Ser.* **75**, 319 (1998). doi:10.1029/AR075p0319
29. M. P. Schodlok, D. Menemenlis, E. Rignot, M. Studinger, Sensitivity of the ice shelf ocean system to the sub-ice shelf cavity shape measured by NASA IceBridge in Pine Island Glacier, West Antarctica. *Ann. Glaciol.* **53**, 156 (2012). doi:10.3189/2012AoG60A073
30. G. D. Williams *et al*., Late winter oceanography off the Sabrina and BANZARE coast (117–1281°E), East Antarctica. *Deep Sea Res. Part II Top. Stud. Oceanogr.* **58**, 1194 (2011). doi:10.1016/j.dsr2.2010.10.035
31. P. R. Holland, A. Jenkins, D. Holland, Ice and ocean processes in the Bellingshausen Sea, Antarctica. *Geophys. Res. Lett.* **115**, (C5), C05020 (2010). doi:10.1029/2008JC005219
32. L. Padman *et al*., Oceanic controls on the mass balance of Wilkins Ice Shelf, Antarctica. *J. Geophys. Res.* **117**, (C1), C01010 (2012). doi:10.1029/2011JC007301
33. P. R. Holland, H. F. J. Corr, D. G. Vaughan, A. Jenkins, P. Skvarca, Marine ice in Larsen Ice Shelf. *Geophys. Res. Lett.* **36**, L11604 (2009). doi:10.1029/2009GL038162
34. P. R. Holland, A. Jenkins, D. M. Holland, The response of ice shelf basal melting to variations in ocean temperature. *J. Clim.* **21**, 2558 (2008). doi:10.1175/2007JCLI1909.1
35. H. H. Hellmer, F. Kauker, R. Timmermann, J. Determann, J. Rae, Twenty-first-century warming of a large Antarctic ice-shelf cavity by a redirected coastal current. *Nature* **485**, 225 (2012). doi:10.1038/nature11064 Medline
36. T. A. Scambos, T. M. Haran, M. A. Fahnestock, T. H. Painter, J. Bohlander, MODIS-based Mosaic of Antarctica (MOA) data sets: Continent-wide surface morphology and snow grain size. *Remote Sens. Environ.* **111**, 242 (2007). doi:10.1016/j.rse.2006.12.020
37. R. A. Bindschadler *et al*., Getting around Antarctica: New high-resolution mappings of the grounded and freely-floating boundaries of the Antarctic Ice Sheet created for the International Polar Year. *The Cryosphere* **5**, 569 (2011). doi:10.5194/tc-5-569-2011
38. J. Mouginot, B. Scheuchl, E. Rignot, Mapping of ice motion in Antarctica using synthetic-aperture radar data. *Remote Sens.* **4**, 2753 (2012). doi:10.3390/rs4092753
39. R. J. Motyka, L. Hunter, K. A. Echelmeyer, C. Connor, Submarine melting at the terminus of a temperate tide-water glacier, LeConte Glacier, Alaska. *Ann. Glaciol.* **36**, 57 (2003). doi:10.3189/172756403781816374
40. E. Rignot, M. Koppes, I. Velicogna, Rapid submarine melting of the calving faces of west Greenland glaciers. *Nat. Geosci.* **3**, 187 (2010). doi:10.1038/ngeo765
41. A. J. Fox, A. Paul, R. Cooper, Measured properties of the Antarctic Ice Sheet derived from the SCAR Antarctic digital database. *Polar Rec. (Gr. Brit.)* **30**, 201 (1994). doi:10.1017/S0032247400024268
42. A. J. Cook, D. G. Vaughan, Overview of areal changes of the ice shelves on the Antarctic Peninsula over the past 50 years. *The Cryosphere* **4**, 77 (2010). doi:10.5194/tc-4-77-2010
43. T. Gammelsrød *et al*., Distribution of water masses on the continental shelf in the southern Weddell Sea, in *The Polar Oceans and Their Role in Shaping the Global Environment, Geophys. Monogr. Ser.*, vol. 85, O. M. Johannessen, R. D. Muench, J. E. Overland (Eds.), pp. 159–176 (AGU, Washington, D. C., 1994), pp.

159–176; doi:10.1029/GM085p0159.
44. P. Schlosser *et al*., Oxygen 18 and helium as tracers of ice shelf water and water/ice interaction in the Weddell Sea. *J. Geophys. Res.* **95**, (C3), 3253 (1990). doi:10.1029/JC095iC03p03253
45. A. S. Shepherd *et al*., Recent loss of floating ice and the consequent sea level contribution. *Geophys. Res. Lett.* **37**, L13503 (2010). doi:10.1029/2010GL042496
46. R. H. Thomas *et al*., A comparison of Greenland ice-sheet volume changes derived from altimetry measurements. *J. Glaciol.* **54**, 203 (2008). doi:10.3189/002214308784886225
47. E. J. Rignot, Fast recession of a west Antarctic glacier. *Science* **281**, 549 (1998). doi:10.1126/science.281.5376.549 Medline
48. A. J. Payne *et al*., Numerical modeling of ocean-ice interactions under Pine Island Bay's ice shelf. *J. Geophys. Res.* **112**, (C10), C10019 (2007). doi:10.1029/2006JC003733
49. C. S. M. Doake, Glaciological Evidence: Antarctic Peninsula, Weddell Sea; *Glaciers, Ice Sheets, and Sea Level: Effect of a CO2-induced Climatic Change*, Seattle Workshop, Washington, 13-15 Sep 1984, USDOE/ER/60235-1, 197-209, (1985)
50. S. S. Jacobs, H. H. Hellmer, A. Jenkins, Antarctic ice sheet melting in the southeast Pacific. *Geophys. Res. Lett.* **23**, 957 (1996). doi:10.1029/96GL00723
51. R. Gerdes, J. Determann, K. Grosfeld, Ocean circulation beneath Filchner-Ronne Ice Shelf from three-dimensional model results. *J. Geophys. Res.* **104**, (C7), 15,827 (1999). doi:10.1029/1999JC900053
52. K. W. Nicholls *et al*., Water mass modification over the continental shelf north of Ronne Ice Shelf, Antarctica. *J. Geophys. Res.* **108**, (C8), 3260 (2003). doi:10.1029/2002JC001713
53. A. Jenkins, D. G. Vaughan, S. S. Jacobs, H. H. Hellmer, J. R. Keys, Glaciological and oceanographic evidence of high melt rates beneath Pine Island Glacier, West Antarctica. *J. Glaciol.* **43**, 114 (1997).
54. H. H. Hellmer, S. S. Jacobs, A. Jenkins, Oceanic erosion of a floating Antarctic glacier in the Amundsen Sea. *Antarct. Res. Ser.* **75**, 83 (1998). doi:10.1029/AR075p0083
55. A. Shepherd, D. Wingham, E. Rignot, Warm ocean is eroding West Antarctic Ice Sheet. *Geophys. Res. Lett.* **31**, L23402 (2004). doi:10.1029/2004GL021106
56. R. A. Bindschadler, D. G. Vaughan, P. Vornberger, Variability of basal melt beneath the Pine Island Glacier ice shelf, West Antarctica. *J. Glaciol.* **57**, 581 (2011). doi:10.3189/002214311797409802
57. P. Heimbach, M. Losch, Adjoint sensitivities of sub-ice-shelf melt rates to ocean circulation under the Pine Island Ice Shelf, West Antarctica. *Ann. Glaciol.* **53**, 59 (2012). doi:10.3189/2012/AoG60A025
58. T. Hughes, The Stability of the West Antarctic Ice Sheet: What has happened and what will happen, *Proceedings, Carbon Dioxide Research Conference: CO2, Science and Consensus*, Berkeley Springs Workshop, 19-23 Sep 1982, USDOE, 820970-021, DE-AC05-76OR00033, 021, IV.62 (1983).

Acknowledgments: We thank three anonymous reviewers for their constructive criticism of the manuscript. This work was performed at the University of California Irvine and at the Jet Propulsion Laboratory, California Institute of Technology under grants from NASA's Cryospheric Science Program and Operation IceBridge (OIB), and at the Lamont-Doherty Earth Observatory of Columbia University under grants from the National Science Foundation and the National Oceanic and Atmospheric Administration.

Supplementary Materials
www.sciencemag.org/cgi/content/full/science.1235798/DC1
Supplementary Text
Figs. S1 to S4
Tables S1 and S2
References (*36–58*)

29 January 2013; accepted 31 May 2013
Published online 13 June 2013
10.1126/science.1235798

Table 1. Meltwater production of Antarctic ice shelves, with ice shelves named counter clockwise in Fig. 1. Areas in square kilometers exclude ice rises and islands. Grounding line flux (GL), surface mass balance (SMB), ice-front (proxy for calving) flux (Ice Front), ice-shelf mass gain ($\partial H/\partial t$ in water mass equivalent), and basal meltwater production in gigatons (1 Gt = 10^{12} kg) per year, with area-average basal melt rate in meter of water per year indicated in parenthesis. Total Antarctica on the last row includes non-surveyed coastal sectors. Ice shelf names are from United States Geological Survey and (*3*). Surveyed ice-shelf mass loss of 287 ± 89 Gt/year in 2003–2008 ($\partial H/\partial t$) is 28 ± 9% higher than that required to maintain the ice shelves in steady state for 2003–2008. *, Larsen B data (velocity, thickness) prior to the 2002 collapse; thinning rate from the remnant part of the ice shelf only. Additional details in table S1.

Name	**Area km^2**	**GL Gt/year**	**SMB Gt/year**	**Ice front Gt/year**	**$\partial H/\partial t$ Gt/year**	**Basal melt Gt/year (m/year)**
Larsen G	412	0.9 ± 0.2	0.1 ± 0	0.7 ± 1	0.0 ± 0	0.3 ± 0.2 (0.71 ± 0.6)
Larsen F	828	1.5 ± 0.3	0.3 ± 0.1	0.6 ± 1	-0.7 ± 0.5	1.2 ± 0.4 (1.4 ± 0.5)
Larsen E	1,184	3.6 ± 0.7	0.4 ± 0.1	1.5 ± 1	1.1 ± 0.7	1.4 ± 1 (1.2 ± 0.9)
Larsen D	22,548	18.5 ± 4	9.8 ± 2	6.3 ± 1	20.5 ± 14	1.4 ± 14 (0.1 ± 0.6)
Larsen C	46,465	29.6 ± 3	23.8 ± 4	31.3 ± 3	1.4 ± 67	20.7 ± 67 (0.4 ± 1)
Larsen B*	6,755	13.6 ± 3	3.0 ± 0.6	8.9 ± 1	-4.5 ± 13	12.2 ± 14 (1.8 ± 2)
Wordie	277	13.8 ± 1	0.3 ± 0	7.6 ± 3	-0.1 ± 0	6.5 ± 3 (23.6 ± 10)
Wilkins	12,866	7.8 ± 2	8.3 ± 2	0.7 ± 0.4	-3.4 ± 16	18.4 ± 17 (1.5 ± 1)
Bach	4,579	5.4 ± 1	1.8 ± 0.3	0.8 ± 0.2	-4.0 ± 0.3	10.4 ± 1 (2.3 ± 0.3)
George VI	23,434	68.2 ± 5	12.7 ± 2	5.7 ± 1.2	-13.8 ± 16	89.0 ± 17 (3.8 ± 0.7)
Stange	8,027	21.0 ± 3	6.0 ± 1	4.6 ± 0.8	-5.6 ± 5	28.0 ± 6 (3.5 ± 0.7)
Ant. Peninsula	127,375	184 ± 26	66 ±13	69 ± 13	-9 ± 74	191 ± 80 (1.5 ± 0.6)
Ronne	338,887	156.1 ± 10	59.3 ± 11	149.2 ± 22	-47.4 ± 22	113.5 ± 35 (0.3 ± 0.1)
Ferrigno	117	11.2 ± 1	0.16 ± 0	6.6 ± 2	-0.3 ± 0	5.1 ± 2 (43.4 ± 17)
Venable	3,194	14.6 ± 2	3.5 ± 1	6.5 ± 1	-7.7 ± 1	19.4 ± 2 (6.1 ± 0.7)
Abbot	29,688	34.0 ± 4	25.0 ± 5	2.4 ± 0.5	4.7 ± 18	51.8 ± 19 (1.7 ± 0.6)
Cosgrove	3,033	5.2 ± 1	1.5 ± 0.3	1.3 ± 1.2	-3.1 ± 2	8.5 ± 2 (2.8 ± 0.7)
Pine Island	6,249	126.4 ± 6	4.6 ± 0.9	62.3 ± 5	-33.2 ± 2	101.2 ± 8 (16.2 ± 1)
Thwaites	5,499	113.5 ± 4	4.8 ± 0.9	54.5 ± 5	-33.7 ± 3	97.5 ± 7 (17.7 ± 1)
Crosson	3,229	27.4 ± 2	3.7 ± 0.7	11.7 ± 2	-19.2 ± 1	38.5 ± 4 (11.9 ± 1)
Dotson	5,803	28.4 ± 3	5.7 ± 1	5.5 ± 0.7	-16.6 ± 2	45.2 ± 4 (7.8 ± 0.6)
Getz	34,018	96.7 ± 5	34.2 ± 7	53.5 ± 2	-67.6 ± 12	144.9 ± 14 (4.3 ± 0.4)
Land	640	14.5 ± 1	0.8 ± 0.1	12.2 ± 1	-0.7 ± 0.3	3.8 ± 1 (5.9 ± 2)
Nickerson	6,495	7.8 ± 1	4.6 ± 0.9	4.3 ± 0.6	3.9 ± 1	4.2 ± 2 (0.6 ± 0.3)
Sulzberger	12,333	15.1 ± 2	8.2 ± 2	1.0 ± 0.2	4.1 ± 2	18.2 ± 3 (1.5 ± 0.3)
Swinburne	900	4.9 ± 0.4	0.9 ± 0.2	1.5 ± 0.3	0.6 ± 0.2	3.8 ± 0.5 (4.2 ± 0.6)
Withrow	632	1.3 ±0.2	0.3 ± 0.0	1.2 ± 0.3	0.1 ± 0.1	0.3 ± 0.4 (0.5 ± 0.6)
Ross West	306,105	73.0 ± 4	33.5 ± 6	100.4 ± 8	7.6 ± 17	-1.4 ± 20 (0.0 ± 0.1)
West Antarctica	756,822	730 ± 47	191 ± 36	494 ± 57	-208 ± 36	654 ± 89 (0.9 ± 0.1)
Ross East	194,704	56.1 ± 4	31.0 ± 6	45.9 ± 4	-7.8 ± 11	49.1 ± 14 (0.3 ± 0.1)
Drygalski	2,338	9.6 ± 0.6	0.3 ± 0.1	3.0 ± 1	-0.8 ± 0.4	7.6 ± 1 (3.3 ± 0.5)
Nansen	1,985	1.3 ± 0.5	0.3 ± 0.1	0.2 ± 0.1	0.4 ± 0.1	1.1 ± 0.6 (0.6 ± 0.3)
Aviator	785	1.1 ± 0.2	0.2 ± 0.	0.2 ± 0.1	-0.3 ± 0.1	1.4 ± 0.2 (1.7 ± 0.3)
Mariner	2,705	2.5 ± 0.4	1.1 ± 0.2	0.6 ± 0.2	0.6 ± 0.3	2.4 ± 0.6 (0.9 ± 0.2)
Lillie	770	3.6 ± 0.3	0.2 ± 0.	0.5 ± 0.1	0.0 ± 0.	3.4 ± 0.3 (4.4 ± 0.4)
Rennick	3,273	4.8 ± 1	0.7 ± 0.1	0.8 ± 0.2	-2.3 ± 0.9	7.0 ± 1 (2.2 ± 0.3)
Cook	3,462	36.0 ± 3	1.7 ± 0.3	27.6 ± 3	5.5 ± 1	4.6 ± 5 (1.3 ± 1)
Ninnis	1,899	27.6 ±2	1.3 ± 0.2	24.6 ± 3	2.0 ± 0.9	2.2 ± 3 (1.2 ± 2)
Mertz	5,522	20.0 ± 1	3.6 ± 0.7	12.0 ± 2	3.6 ± 1	7.9 ± 3 (1.4 ± 0.6)
Dibble	1,482	12.5 ± 1	1.5 ± 0.3	8.2 ± 0.9	-2.3 ± 0.7	8.1 ± 1 (5.5 ± 0.9)
Holmes	1,921	26.0 ± 2	2.8 ± 0.5	24.7 ± 4	-2.5 ± 1	6.7 ± 4 (3.5 ± 2)
Moscow Univ.	5,798	52.3 ± 1	4.7 ± 0.9	29.6 ± 3	-0.1 ± 3	27.4 ± 4 (4.7 ± 0.8)
Totten	6,032	71.0 ± 3	6.2 ± 1	28.0 ± 2	-14.0 ± 2	63.2 ± 4 (10.5 ± 0.7)
Vincennes	935	12.7 ± 1	0.5 ± 0.1	6.8 ± 1	1.3 ± 0.6	5.0 ± 2 (5.3 ± 2)
Conger/Glenzer	1,547	1.7 ± 0.4	0.9 ± 0.2	1.1 ± 0.8	-2.1 ± 1	3.6 ± 1 (2.3 ± 0.9)
Tracy/Tremenchus	2,845	0.6 ±0.4	1.0 ± 0.2	0.2 ± 0.1	-1.7 ± 2	3.0 ± 2 (1.5 ± 0.7)
Shackleton	26,080	55.0 ± 4	16.2 ± 3	30.3 ± 3	-31.7 ± 14	72.6 ± 15 (2.8 ± 0.6)
West	15,666	41.9 ± 4	6.9 ± 1	32.6 ± 7	-11.1 ± 7	27.2 ± 10 (1.7 ± 0.7)
Publications	1,551	5.8 ± 0.8	0.4 ± 0.1	5.2 ± 1	-0.5 ± 0.8	1.5 ± 2 (1.0 ± 1)
Amery	60,654	56.0 ± 0.5	8.5 ± 2	50.4 ± 8	-21.4 ± 21	35.5 ± 23 (0.6 ± 0.4)
Wilma/Robert/Downer	858	10.3 ±0.5	0.6 ± 0.1	0.8 ± 0.4	0.0 ± 0	10.0 ± 0.6 (11.7 ± 0.7)
Edward VIII	411	4.1 ± 0.8	0.4 ± 0.1	0.3 ± 0.1	0.0 ± 0	4.2 ± 0.8 (10.2 ± 2)
Rayner/Thyer	641	14.2 ± 1	0.3 ± 0.1	7.8 ± 0.6	0.0 ± 0	6.7 ± 1 (10.5 ± 2)
Shirase	821	15.0 ± 1	0.4 ± 0.1	9.6 ± 1	0.0 ± 0	5.7 ± 1 (7.0 ± 2)
Prince Harald	5,392	8.3 ± 1	4.1 ± 0.8	10.3 ± 2	4.0 ± 2	-2.0 ± 3 (-0.4 ± 0.6)
Baudouin	32,952	22.0 ± 3	8.4 ± 2	6.5 ± 1	9.8 ± 11	14.1 ± 12 (0.4 ± 0.4)
Borchgrevink	21,580	19.6 ± 3	6.1 ± 1	17.5 ± 3	0.7 ± 4	7.5 ± 6 (0.3 ± 0.3)
Lazarev	8,519	3.7 ± 0.6	2.0 ± 0.4	3.1 ± 1	-3.6 ± 2	6.3 ± 2 (0.7 ± 0.2)
Nivl	7,285	3.9 ± 0.8	1.8 ± 0.3	1.3 ± 0.4	0.6 ± 1	3.9 ± 2 (0.5 ± 0.2)
Vigrid	2.089	2.7 ± 0.4	0.4 ± 0.1	2.0 ± 0.4	-2.0 ± 0.4	3.2 ± 0.7 (1.5 ± 0.3)
Fimbul	40,843	24.9 ± 4	12.7 ± 2	18.2 ± 2	-4.0 ± 7	23.5 ± 9 (0.6 ± 0.2)
Jelbart	10,844	9.9 ± 1	4.9 ± 0.9	8.8 ± 2	6.9 ± 2	-1.0 ± 3 (-0.1 ± 0.3)
Atka	1,969	0.9 ± 0.2	0.8 ± 0.1	1.0 ± 0.2	1.1 ± 0.2	-0.5 ± 0.4 (-0.2 ± 0.2)
Ekstrom	6,872	4.1 ± 0.8	2.6 ± 0.5	2.3 ± 0.6	0.0 ± 0	4.3 ± 2 (0.6 ± 0.2)
Quar	2,156	1.0 ±0.2	0.5 ± 0.1	0.6 ± 0.1	-0.5 ± 0.4	1.4 ± 0.5 (0.7 ± 0.2)
Riiser-Larsen	43,450	21.5 ± 3	12.7 ± 2	12.1 ± 2	13.4 ± 8	8.7 ± 9 (0.2 ± 0.2)
Brunt/Stancomb	36,894	20.3 ± 3	11.4 ± 2	28.1 ± 4	2.6 ± 4	1.0 ± 7 (0.03 ± 0.2)
Filchner	104,253	97.7 ± 6	13.4 ± 2	82.8 ± 4	-13.6 ± 7	41.9 ± 10 (0.4 ± 0.1)
East Antarctica	669,781	782 ± 80	174 ± 33	546 ± 70	-70 ± 34	480 ± 116 (0.7 ± 0.2)
Total surveyed	**1,553,978**	**1,696 ± 146**	**430 ± 81**	**1,089 ± 139**	**-287 ± 89**	**1,325 ± 235 (0.85 ± 0.1)**
Total Antarctica	1,561,402	2,048 ± 149		1,265 ± 141		1,500 ± 237

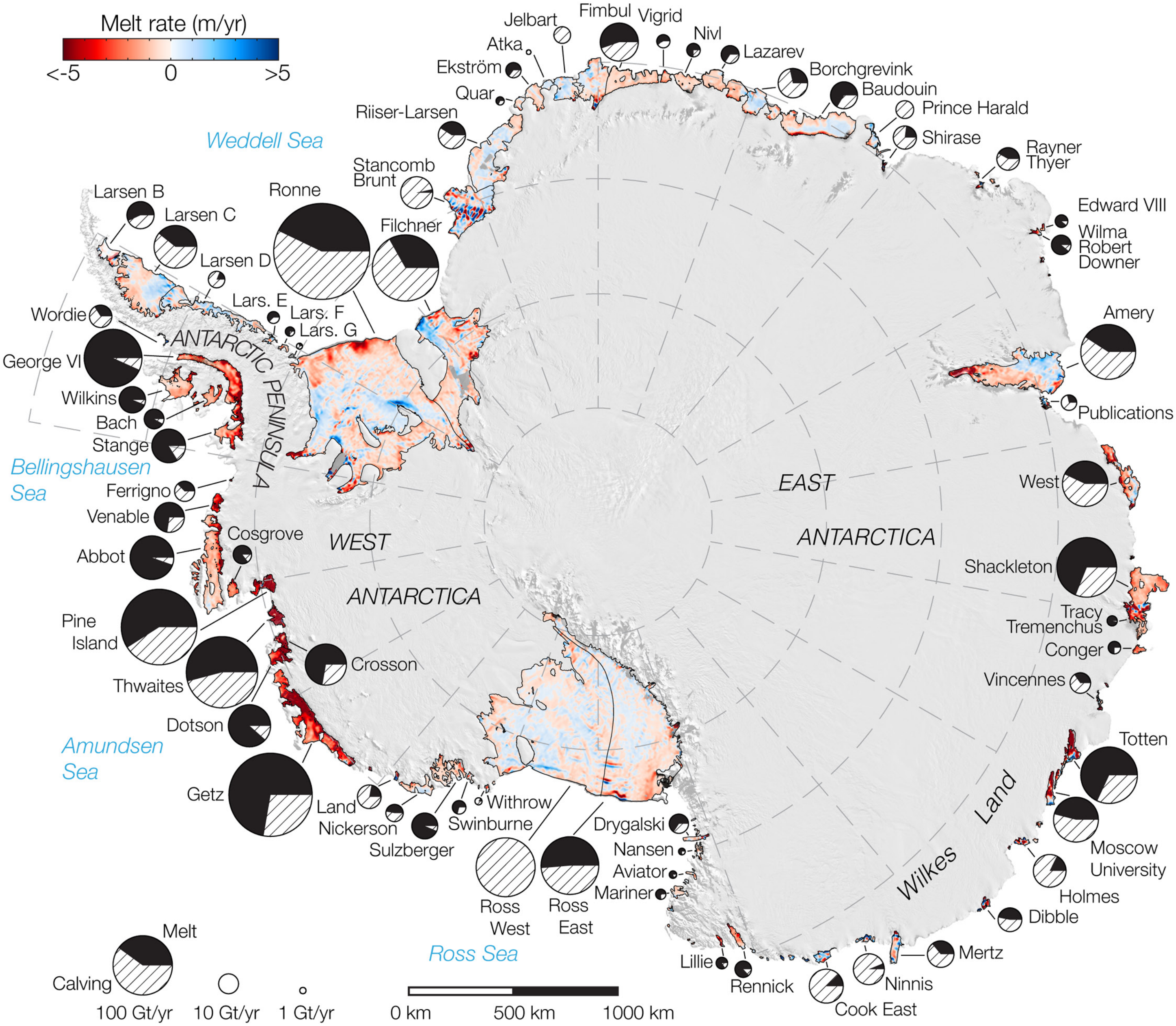

Fig. 1. Basal melt rates of Antarctic ice shelves color coded from < –5 m/year (freezing) to > +5 m/year (melting) and overlaid on a 2009 MODIS mosaic of Antarctica. Ice-shelf perimeters in 2007–2008, excluding ice rises and ice islands, are thin black lines. Each circle graph is proportional in area to the mass loss from each shelf, in gigatons (1 Gt = 10^{12} kg) per year, partitioned between iceberg calving (hatch fill) and basal melting (black fill). See Table 1 and table S1 for additional details on ice shelf locations, areas, and mass balance components.